ADVANCED ELECTROMAGNETICS, VOL. 6, NO. 1, FEBRUARY 2017

Performance Improvement of Ultra Wideband Multiple Access Modulation System using a new Optimal Pulse Shape

Vikas Goyal[1], B.S. Dhaliwal[2]

[1] Department of Electronics and Communication Engineering, Guru Kashi University, Talwandi Sabo, INDIA.
[2] Department of Electronics and Communication Engineering, Guru Kashi University, Talwandi Sabo, INDIA.

*corresponding author, E-mail: vikas312002@yahoo.com

Abstract

Ultra-wideband (UWB) uses very low energy levels to transfer data at very high data rate and bandwidth. An optimal and correct choice of transmission pulse shape is an important criterion in this technology. In this paper, we will present an approach for the generation of an optimal pulse shape with the optimal generation of pulse shape values that can provide effective results when transmitted using multiple access modulation technique over a multipath channel and received by a RAKE type receiver. The bit error analysis of constructed model is also given using Ideal Rake, selective RAKE, and partial RAKE receiver configurations.

Keywords: UWB, PPM, PAM, PAM-TH, RAKE, Multipath.

1. Introduction

Ultra-wideband (UWB) technology is referred to as baseband, carrier-free or impulse technology, used to provide very high data rates at very low power levels for short and medium range communication systems. In 1998, the Federal Communications Commission (FCC) [1] started the transmissions norms. UWB systems with central frequency (f_C) greater than 2.5 GHz requires a bandwidth of at least five hundred MHz, while UWB systems with the central frequency less than 2.5 GHz should have the fractional bandwidth (Bandwidth/central frequency) of at least 0.2 [2][3]. Ultra-wideband communication technology is very useful for communication and remote sensing applications. Due its high bandwidth, it is used for short to medium range wireless applications. The spectrum allocation to ultra wideband systems has been shown in fig.1. For the generation of UWB signals a research paper [4] explained that Impulse radio can be used for ultra wideband transmission using a Gaussian monocycle pulse. Another research paper [5] explained different pulse shapes that can be used for UWB communication systems. Ultra-wideband pulse design method has been proposed that made use of a linear pulse combination waveform of the sub-band signals [11]. A linearly combining two monocycles using different pulse shapes is described in [12] to satisfy the radiated power limits of ultra wideband transmission. A combination of Gaussian derivatives over definite sub bands to increase the power spectrum utilization is described by taking the pulse shaping factors and the number of derivatives by trial and error method for selecting the pulse shaping factors for different Gaussian derivatives to match the emission mask was presented in the article [14]. In Research paper [18], UWB pulses and their respective power spectral efficiency was generated by combining the multiple monocycle pulses of first, second, third and fifth Gaussian derivatives with their inverse polarities to meet the emission mask criteria. Another article [19] presented the pulse design technique based on linear combination of Gaussian doublet pulses and found that their proposed pulse, showed better spectral power efficiency as compared to other conventional pulse shapes. A new UWB pulse shaping method was also presented in [20] that divided the entire spectrum of UWB into different regions, and in each region the Gaussian pulse and its derivatives were combined, using least square error combination technique with same pulse shaping values. IEEE 802.15.3a Channel Model described in [7] [16] for Ultra wideband Indoor Communication. Research paper [8] illustrates direct sequence impulse UWB radio modulation systems. Article [9] [22] presented the applications of the ultra wideband communication systems. Article [10] [15] [23] presented the RAKE receiver with Maximal Ratio Combining for ultra wideband communication systems.

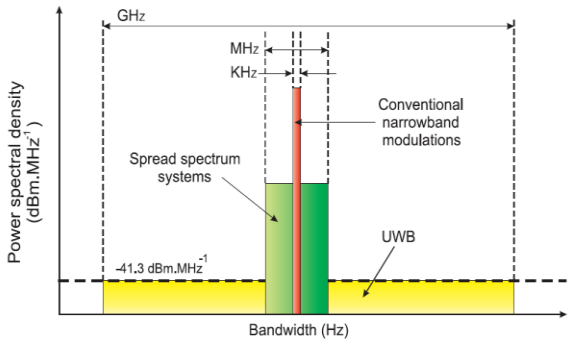

Fig.1. Spectrum allocation of UWB

Effective isotropic radiated power (EIRP) for the ultra wideband systems have been set at −41.3 dBm/MHz for 3.1 to 10.6 GHz as shown in fig.2. Therefore, the pulses used for the generation of UWB signals should follow these limits very closely to get an optimal performance in case of multipath environments.

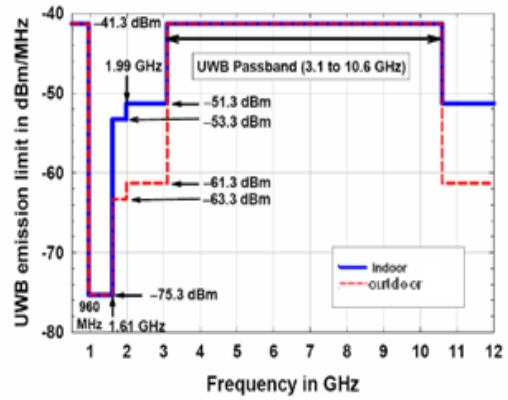

Fig.2. EIRP limits of UWB

2. Signal generation and proposed approach

The pulses used for signal generations meeting the EIRP limits can be obtained by using the standard Gaussian pulses and their higher order derivatives equations [3] given below.

The Gaussian pulse is given as

$$P(t) = \frac{A}{\sqrt{2\pi}\sigma} e^{-\left(\frac{t^2}{2\sigma^2}\right)} \qquad (1)$$

Also, the higher derivative of Gaussian pulse equation can be expressed as:

$$P^{(n)}(t) = -\frac{n-1}{\sigma^2} P^{(n-2)}(t) - \frac{t}{\sigma^2} P^{(n-1)}(t) \qquad (2)$$

Where n is the derivative order, A is the amplitude and σ is the standard deviation related to [3] pulse shape factor ($\alpha = 2\sigma\sqrt{\pi}$).

The PSD of the transmitted signal (PSD_t) is given by the following equation:

$$|PSD_t(f)| = A_{max}|PSD_n(f)|$$

$$= A_{max} \frac{(2\pi f\sigma)^{2n}}{n^n} \frac{e^{-(2\pi f\sigma)^2}}{e^{-n}} \qquad (3)$$

Where Amax is the peak Power Spectral density.

By solving the above equation we can find the optimal values of the Gaussian pulse derivatives that satisfy the UWB emission mask limits.

However, the pulse shapes used for the signal generation to get more improved result can be achieved by combining the higher order derivatives of the Gaussian pulse and using a randomization approach of obtaining the coefficients of the Gaussian derivative pulses which follows the EIRP radiation limits described above very closely .

The combined pulse can be given as

$$P(t) = \sum_{n=1}^{N} C_n P^n(\alpha_n, t) \qquad (4)$$

Where n denotes the derivative order of Gaussian pulse and C_n denotes the set of optimal coefficients.

The steps followed to find the optimal pulse are given below:-

Step1. Generate the set of different Gaussian derivatives (i=1: n)
Step2. Set the number of attempts to find the most optimal coefficient set closely meeting UWB EIRP/emission limits.
Step3. Apply the pulse shape factors to the generated Gaussian derivatives
Step4. Generate the UWB Emission Mask with defined EIRP limits.
Step5. Initialization: - Initialize the random number generator, coefficients set and number of attempts
Step6. Random Generation: - Generate random coefficients set for the Gaussian derivatives
Step7. Generate the combined pulse using the Gaussian derivatives and the generated random set in step 6.
Step8. Find the Power Spectral Density (PSD) of combined Pulse.
Step9. Check whether the obtained PSD of the combined pulse meet the UWB emission mask limits.
Step10. If the emission mask/EIRP limits are not satisfied then repeat the step no.6 and obtain another set of random coefficients otherwise go to step 11.
Step11. If the limits are satisfied, record the set of coefficients and its related Power
Step12. If it is the first obtained set meeting the limits then go to step no.14 otherwise, go to step no. 13.
Step13. Compare the energy of present set with the previous present/recorded set to see which set has the better matching of the emission mask limits. .
Step14. Record the set having the highest energy go to step no. 15.
Step15. Mark the set of coefficients as optimal set C with the highest power.
Step16. Go to step no.5 for another attempt and repeat the process to obtain the set of coefficients satisfying the limits more closely.
Step17. After running for all attempts we will get the most optimal set of coefficients C having the highest power and meeting the limits very closely.
Step18. Obtain the combined pulse using the most optimal set C.

3. System Model

To reduce the interference from other operating ultra wideband transmissions and provide multiple access capability, a randomizing technique like Time-Hopping (TH) at the transmitter has to be applied, so that the does not interfere with other narrowband signals. In Time hopping, each symbol transmission time is divided into N frames which are further divided into N time slots and each user is assigned a time slot in the frame to transmit. Time hopping (TH) technique changes the time slot from frame to frame according to the user's code. In this way, more energy is allocated to a symbol and the transmission range is increased [27]. In this paper, we will consider the UWB transceiver using time hopping technique in combination with pulse position modulation technique using the proposed optimal combined pulse shapes shown in Fig. 3.

The binary bits with a pseudo random sequence and amplitude modulating them. The binary bits converted into a sequence of binary amplitudes. The adding a user specific pseudo code before sending it to the pulse position modulator where the pulses sequence positioned at jT_s in a specific time hopping slot time according to the code $(c_j T_c)$ along with the pulse shift introduce by pulse position modulator used to modulate the bits. [9][10] The signal at the output of the transmitter is represented as

$$s(t) = \sum_{j=-\infty}^{+\infty} d_j \, p(t - jT_s - c_j T_c - a\, j\varepsilon) \quad (5)$$

Where, Ts is frame time, $c_j T_c$ is time hopping codes hift and $a\, j\varepsilon$ is PPM shift

$$g(t) = S(t)^* h(t) \quad (6)$$

$$r(t) = g(t) + n(t) \quad (7)$$

Where, g(t) is the useful signal at the receiver and n(t) is additive noise assumed to be Gaussian process .

4. UWB Multipath Channel

The output of the transmitter is sent over the ultra wideband multipath channel (IEEE 802.15.3a) [16]. This impulse response of the channel can be of four types (CM1, CM2, CM3 or CM4) with defined user parameters given in table 1.

Table 1. UWB IEEE802.15.3a channel parameters

Channel Characteristics	Case A LOS (0-4m)	Case B NLOS (0-4m)	Case C NLOS (4-10m)	Case D Extreme NLOS
Cluster arrival rate Λ(1/ns)	0.0233	0.4	0.0667	0.0667
Ray arrival rate λ(1/ns)	2.5	0.5	2.1	2.1
Cluster delay factor Γ(1/ns)	7.1	5.5	14.0	24.0
Ray delay factor γ(1/ns)	4.3	6.7	7.9	12.0
Standard deviation of cluster lognormal fading σ_1 (dB)	3.3941	3.3941	3.3941	3.3941
Standard deviation of ray lognormal fading σ_2 (dB)	3.3941	3.3941	3.3941	3.3941
Standard deviation of lognormal shadowing term σ_x (dB)	3	3	3	3

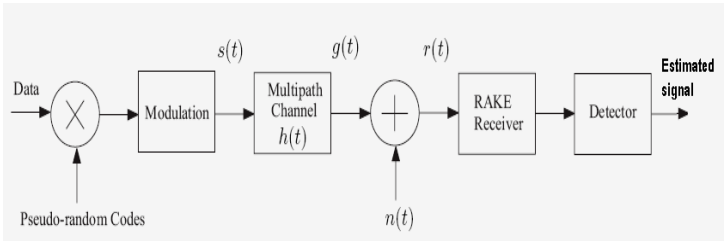

Fig.3. System Model

Where, CM1 used for a line of sight less than 4m, CM2 for non-line of sight less than 4m, CM3 for non-line of sight, 4-10m, and CM4 for greater than 10m [7].

The channel impulse response is given as:-

$$h(t) = \sum_{l-1}^{F} \sum_{n-1}^{P} \alpha_{nl}\ \delta(t - T_l - \tau_{nl}) \quad (8)$$

Where a number of clusters are represented by F and the paths within the group are represented by P. α_{nl} denotes the nth multipath gain. T_l and τ_{nl} give the delay.

5. Receiver

Transmitted signal through the channel is received by rake receiver. The rake receiver [6] shown in Fig.5 consists of a matched filter that is matched to the transmitted waveform and a tapped delay line that matches with the impulse response of the channel. It uses correlators and delays to spread out the individually delayed multipath signals. Every signal is delayed as per the peaks founded in the received signal. Then each component is separately coded and combined at the end using a maximum ratio combining technique in which the outputs of the correlator are weighted and each branch signal is multiplied with weighting factor (proportional to the signal amplitude) so that the outputs

responding to strong signals are given more weight than the weak signals to have higher signal to noise ratio (SNR) in a multipath environment. Based on this the estimated combined signals are found out by the detector.

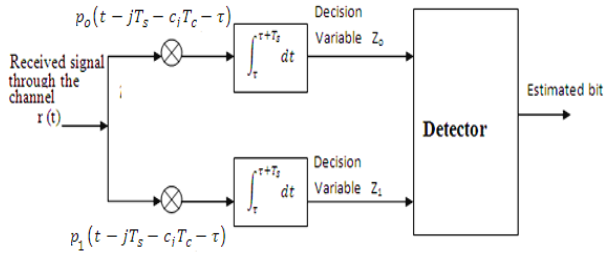

Fig.4. Receiver structure for the system model

The correlation mask can be expressed as

Mask = $p_o(t - \tau - c_jT_c)$ *and* $p_o(t - \tau - c_jT_c - a_j\varepsilon)$

Where $p_o(t - \tau - c_jT_c)$ *and* $p_o(t - \tau - c_jT_c - a_j\varepsilon)$ are the correlation signals used to match the transmission signal for binary bit 0 and bit 1 with pulse shift respectively.

Fig.4 describes the Receiver structure used for the system model using pulse position modulation and time hopping multiple access technique where the received signal delayed multipath components are correlated with the transmitted signal.

The receiver configurations [13] considered are the Ideal or All RAKE which considers all the multipath delay components, Selective RAKE selects the best paths from all the multipaths and Partial RAKE takes the first arrived multipath into consideration.

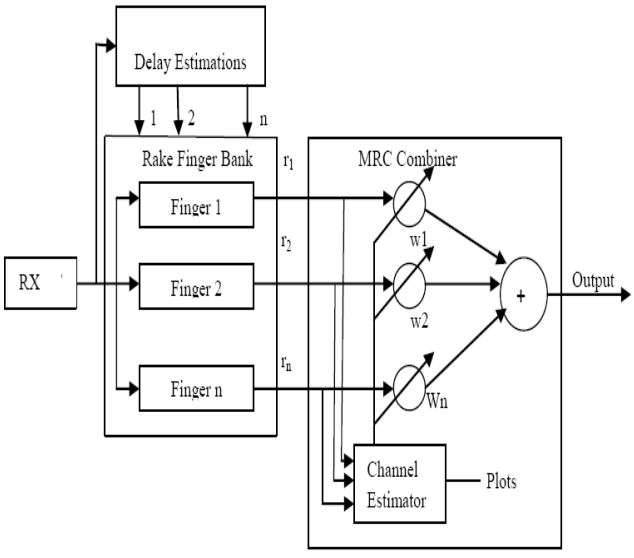

Fig.5. RAKE Receiver

6. Simulation Results and Discussions

The above- described method of generating an optimal pulse described in the proposed method is created and simulated using Matlab software.

Using the bisection method, we can find the optimal values of pulse shape values by finding the roots of above equation for higher order derivatives of Gaussian pulse.

Table 2. Optimal Pulse shape factors values

Derivative	Pulse shape value(α) in seconds (s)	Peak Frequency (GHz.)
First	0.1162×10^{-9}	4.885
Second	0.1363×10^{-9}	5.886
Third	0.1522×10^{-9}	6.387
Fourth	0.1657×10^{-9}	6.887
Fifth	0.177×10^{-9}	7.139
Sixth	0.1887×10^{-9}	7.389
Seventh	0.1988×10^{-9}	7.515

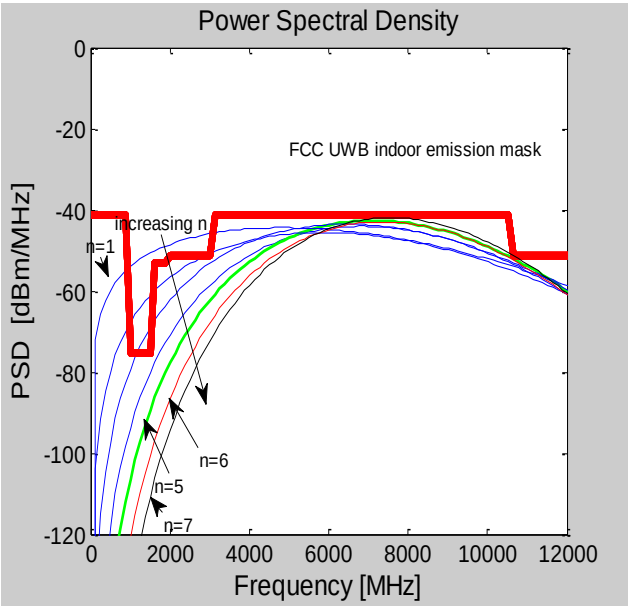

Fig.6. Power Spectral density of the Gaussian derivatives for obtained pulse shape values

It is found that the PSD of 5th order Gaussian derivative shown by green curve closely fits the UWB emission mask as compared to the other derivatives. Therefore, we take 5th order derivative of Gaussian pulse as standard pulse and

consider up to 5th derivatives for making an optimal combined pulse in our experimental work.

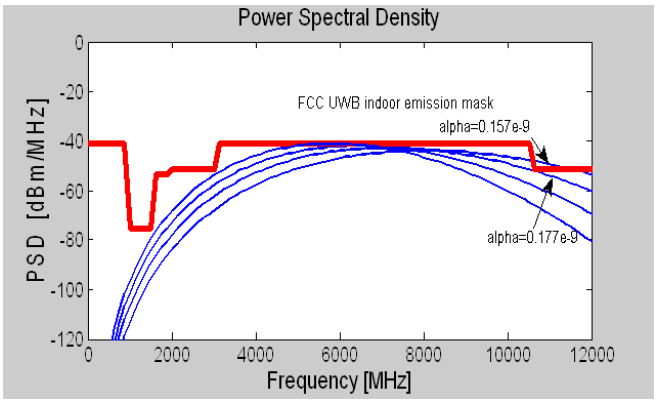

Fig.7. PSD for 5th derivative Gaussian Pulse

Fig. 7 shows the fifth optimal derivative of Gaussian pulse with the obtained pulse shape factor value of 0.177 × 10^{-9}s given in Table 2 matches the emission mask more closely as compared to the other nearby taken values of the pulse shaping factors of 0.157 × 10^{-9}s, 0.197 × 10^{-9}s, 0.217 × 10^{-9}s which shows that the obtained pulse shape factor value is optimal and are in accordance with the EIRP emission mask limits.

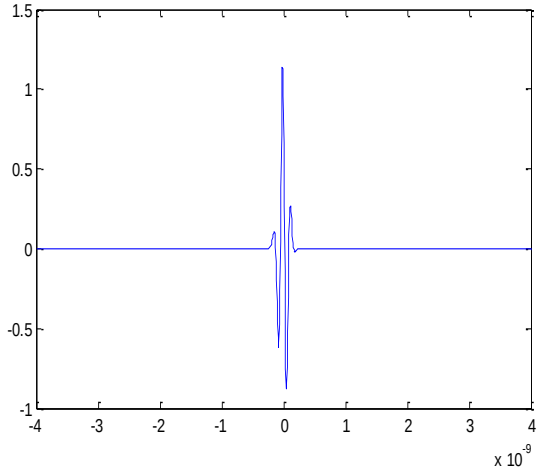

Fig.8. Optimal Pulse

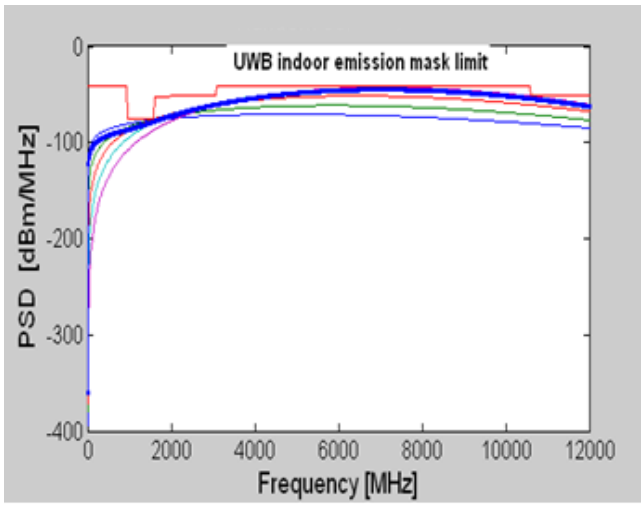

Fig.9. Optimal pulse shape Power Spectral Density

Fig.8. shows the generated optimal pulse using proposed approach using optimal values of [0.1162e-9, 0.1363e-9, 0.1522e-9 ,0.1657e-9 and 0.1778e-9] and obtained optimal coefficients C_n = [0.0260 -0.1610 -0.0835 -0.8350 0.7625]. Fig.9 shows that the power spectral density(PSD) of the optimal pulse shown by dark blue curve following the emission limit requirements effectively as compare to the individual PSD of the first five derivatives using optimal values given in table 2 with the power spectral utilization (ratio of the spectral power of the pulse transmitted and the spectral power of the emission mask in 3.1GHz to 10.6 GHz frequency range) of nearly 85% as compared to the results presented in [14] with the shaping factor selected by trial and error method as 1.5 x 10^{-9}s for first derivative and 0.35 x 10^{-9}s for second to fifteen derivatives The results obtained by our method using optimal pulse values also shows significant improvement as compared to the proposed pulse and fifth-order derivative with spectral efficiency of 57.40% by linear combination of Gaussian doublet pulses in [19], the power spectral utilization of 35 % and 48.52% stated for the pulse in [21] and about 60-70% by the combination of Gaussian pulse and its derivatives in [24]. The obtained optimal pulse shows better results as compared to results presented in paper [12] by linearly combining two first-order derivatives of Gaussian pulses using different pulse shaping values of 0.049ns and 0.048ns . Also, the emission matching attained by our proposed method shows an improvement using the optimal pulse factor values for the first five Gaussian derivatives as compared to the same pulse factor value of 0.7 ns for the derivatives given in [20].

In our analysis for the channel model we have considered CM3 parameters given in the table 1 and obtained the channel impulse response shown in Fig.10.

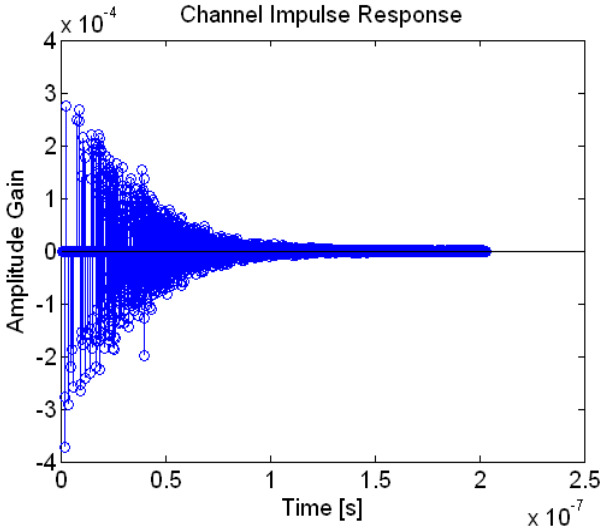

Fig.10. Channel Impulse response of UWB CM3

The Ultra wideband transceiver model is also simulated using the above pulse and standard Gaussian pulse fifth derivate for Time hopping pulse position multiple access modulation system in the multipath channel environment to calculate the bit error rate (BER) for one thousand transmission bits using sample frequency of 50 x 10^9 Hz, transmission power of -30dBm, using five pulses per bit for transmission of hundred bits and each pulse having 0.5 x 10^{-9}s, PPM shift 0.5 x 10^{-9}s, frame duration of 5 x 10^{-9} s and five Time slots per frame.

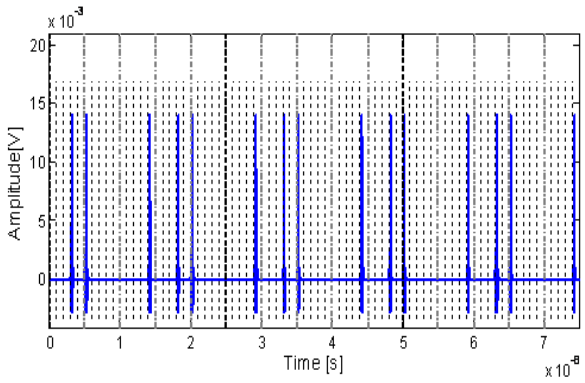

Bit 1 0 1

Fig.11. Reference transmitted signal using fifth derivative Gaussian pulse

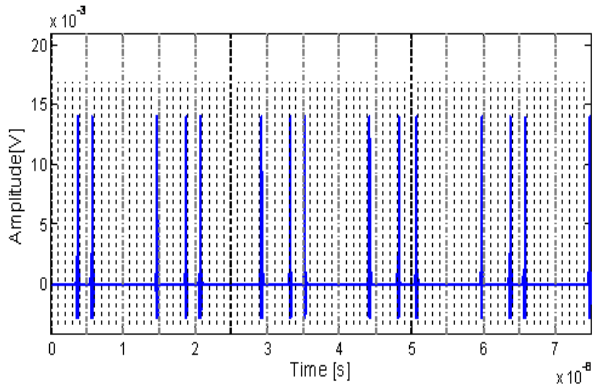

Bit 1 0 1

Fig.12. Transmitted signal using fifth derivative Gaussian pulse after Modulation

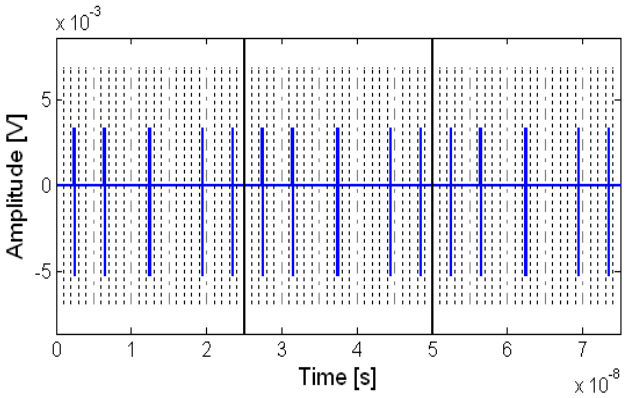

Bit 1 0 1

Fig.13. Reference transmitted signal using optimal pulse

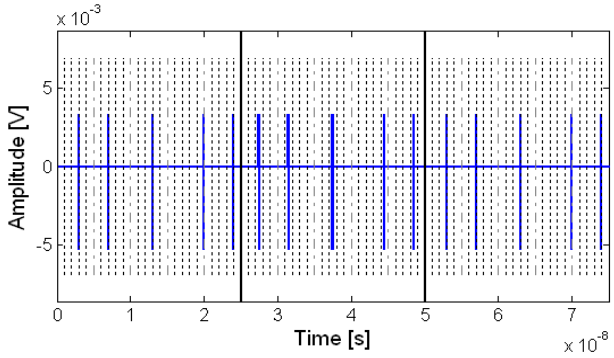

Bit 1 0 1

Fig.14. Transmitted signal using optimal pulse after Modulation

Fig.11 and Fig.13 show the generation of transmitted reference signal before modulation and Fig.12 and Fig.14 shows the transmitted signal after modulation using the using the fifth derivative Gaussian pulse and proposed

method of pulse combining respectively using binary pulse position modulation time hopping technique.

Here, the bits are transmitted and five pulses are used for every transmitted bit. The total time frame duration (25 x 10^{-9} s) of each bit is divided into five-time slots and only one pulse is transmitted successfully in each time slot shows a perfect generation of time hopping signals.

The modulated signal in Fig.12 and Fig.14 shows a pulse position shift of 0.5 x 10^{-9} s for the transmitted bit 1 used to modulate the reference combined signal. The pulse shift is clearly visible for every binary bit 1 to be transmitted and no pulse shift is observed for the transmission of binary bit 0. From the above figures, we can conclude that a perfect transmission signal is generated using our proposed approach of pulse combining.

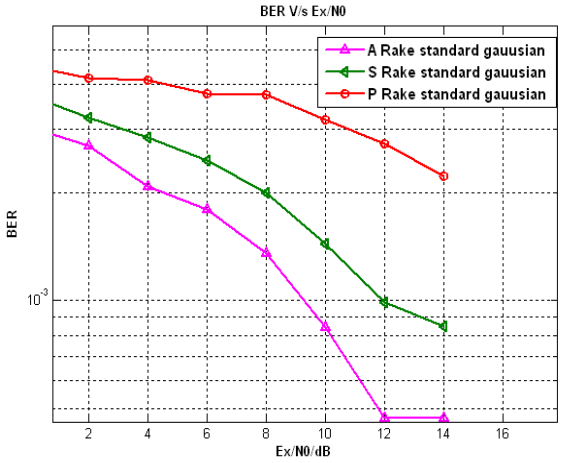

Fig.15. BER Analysis of System Model for the standard Gaussian fifth derivative using optimal coefficients

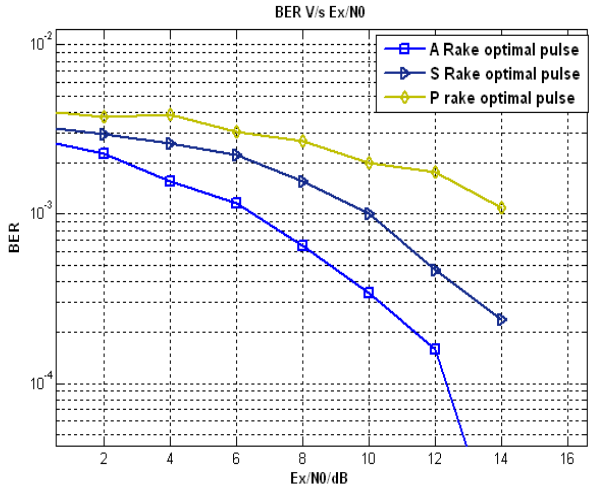

Fig.16. BER Analysis of System Model for the optimal pulse using optimal coefficients

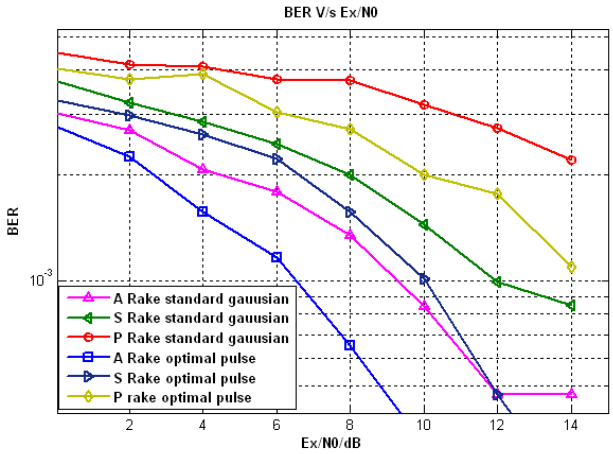

Fig.17. BER Comparison of optimal pulse and the standard Gaussian pulse.

The rake receiver results are plotted as bit error rate (BER) versus energy per bit to noise power spectral density ratio (normalized signal to noise ratio) in decibel (Ex/No dB) results are obtained for the standard gaussian derivative pulse shape described in equation no.3 and the proposed combined pulse shape after passing the transmitted signal through UWB channel model CM3.The results are obtained for Ideal rake, selective rake, and Partial rake receiver configurations. The results obtained above in terms of bit error rates at different normalized signal to noise ratio (Ex/No dB) values are given in table 3.

Table3. Bit error rates at different normalized signal to noise ratio (Ex/No dB) values

UWB Pulse	Receiver Configu--ration	BER at different (Ex/No) dB values		
		0dB	6dB	10dB
UWB System Using Standard Gaussian Pulse	A Rake	3.02×10^{-3}	1.79×10^{-3}	8.4×10^{-4}
	S Rake	3.72×10^{-3}	2.46×10^{-3}	1.44×10^{-3}
	P Rake	4.51×10^{-3}	3.77×10^{-3}	3.18×10^{-3}
UWB System Using Optimal pulse	A Rake	2.76×10^{-3}	1.16×10^{-3}	3.4×10^{-4}
	S Rake	3.29×10^{-3}	2.23×10^{-3}	1.01×10^{-3}
	P Rake	4.04×10^{-3}	3.04×10^{-3}	2.03×10^{-3}

Based on the BER Simulation results of standard Gaussian derivative pulse and the optimal pulse using pulse shape factors shown in fig.15 and fig.16 respectivly and the BER comparison results shown in fig.17, we can see that the Ideal (A rake) shown sky blue curve, selective rake shown by the dark blue curves and partial rake receiver shown by golden curve for the optimal proposed pulse shows better performance in terms of the bit error rate over the Ideal (A rake) shown sky pink curve, selective rake shown by the green curves and partial rake receiver shown by red curve for gaussian fifth derivative with opimal pulse factors

respectively. The results obtained above also shows significant improvement in terms of bit error rates at the higher values of (Ex/No/ dB) and are better in comparison to the results presented in [26] and [28] for the multiple access modulated system over the multipath channel. The Also, the above results obtained for the selective Rake and Partial rake receiver configurations with two branches show that the ultra wideband system using proposed combined pulse shapes performs better than the gaussian derivative pulse shape generally used by the researchers to generate the transmission signal as in paper [15] and [23].

7. Conclusion

In this paper, we proposed a method to obtain an optimal pulse shape following very closely the prescribed EIRP limits using first five Gaussian derivative pulses with optimal shaping factors as basic functions. The pulse generated with the channel coefficients and pulse shaping factors follows the power spectral density requirements of an ultra wideband signal closely as compared to the previous literature results. The system model using pulse position modulation time hopping is generated using binary modulation and optimal pulse shape in multipath channel environments and the bit error rate results obtained in Fig. 17.shows that the proposed optimal combined Pulse shape gives an improved performance over the optimal Gaussian fifth derivative pulse system for all the three receiver configurations considered. This optimal pulse can be used as a reference for achieving improved results in multipath channel environments.

References

[1] Federal Communications Commission. Revision of Part 15 of the Commission's Rules Regarding Ultra-Wideband Transmission Systems, "First Report and Order, *FCC 02*, vol. 48, pp. 1-89, 2002.

[2] V. Goyal, Vikas, Pulse Generation and Analysis of Ultra Wide Band System Model, *Computer Science & Telecommunications*, 2 (34):3-6, 2012.

[3] V. Goyal, B.S. Dhaliwal, Optimal Pulse Generation for the improvement of ultra wideband system performance, *Proc. IEEE International Conference on Recent Advances in Engineering and Computational Sciences (RAECS)*, pp. 1-6, 2014.

[4] T. Ali, P. Siddiqua, M. A. Matin, Performance evaluation of different modulation schemes for ultra wide band systems, *Journal of ELECTRICAL ENGINEERING*, 65: 184–188, 2014.

[5] B. Lin, G. Cai, M. Zhuang, Capacity comparison of UWB system based on combined Cosinusoid Gaussian pulse, *Proc. IEEE International Conference on Anti-Counterfeiting, Security and Identification (ASID),* pp. 93- 96, 2011.

[6] X. Zuo, D. Wang, R. Yao, RAKE reception for IR-UWB systems in high mobile environments, *in Proc. International Conference on Systems and Informatics(ICSAI)*, pp. 1459-1462, 2012.

[7] J R. Akbar, E. Radoi, An overview of synchronization algorithms for IR-UWB systems," in *Proc. International Conference on Computing, Networking and Com-munications (ICNC)*, pp. 573-577, 2012.

[8] V. Goyal, B.S. Dhaliwal, Ultra Wideband PAM Modulation and Reception in UWB Multi Path channel Using Rake Configurations, *Computer Science & Telecommunications*, 45: 71-76 2015.

[9] V. Goyal, B.S. Dhaliwal, Ultra Wideband Pulse Modulation System in Comparison to Conventional Narrowband Wireless Systems." *in Proc. Of 19th Punjab Science Congress, S.U.S Group of Institutes, Tangori,* pp. 179-180, 2016.

[10] H. Zhang, G. T. Aaron, "Performance and Capacity of PAM and PPM UWB Time-Hopping Multiple Access Communications with Receive Diversity," *EURASIP Journal on Advances in Signal Processing*, 3: 1-10, 2005.

[11] Bin Li, Zheng Zhou, Weixia Zou, Dejian Li, Chong Zhao, Optimal waveforms design for ultra-wideband impulse radio sensors, *Sensors* 10,12: 11038-11063, 2010.

[12] M. J. Koonen, Novel generation and transmission of 2 Gbps impulse radio ultra wideband over MMF for in-building networks application." *In Proc. Of IEEE Conference on Optical Fiber Communication (OFC), collocated National Fiber Optic Engineers Conference, (OFC/NFOEC),* pp. 1-3, 2010.

[13] Randall Tombaugh, A RAKE Receiver Employing Maximal Ratio Combining (MRC) Without Channel Estimation for UWB Communications, *The Osprey Journal of Ideas and Inquiry*, All Volumes (2001-2008), paper 45, 2007.

[14] L. Li, P. Wang, X. d. Wu, J. Zhang, Improved UWB pulse shaping method based on Gaussian derivatives, Wireless Mobile and Computing (CCWMC 2011), *Proc. Of IET International Communication Conference*, Shanghai, pp. 438-442, 2011.

[15] K. Xiao-fei, L.Bai-ping, The BER performance analysis and simulation of rake receiver for UWB systems." *Proc. IEEE Workshop on Advanced Research and Technology in Industry Applications*, pp. 267-269, 2014.

[16] J.R.Foerster, Channel modelling sub-committee report, IEEE 802.15 Working Group for Wireless Personal Area Networks (WPANs), *IEEE P802*, pp.15-02, 2003.

[17] V. Goyal, B.S. Dhaliwal, Ultra Wideband Pulse Generation Using Multiple Access Modulation Schemes, *International Journal of Engineering Sciences & Research Technology*, 4: 53-59, 2015.

[18] Li. Pengxiao, C. Hongwei, C, Minghua, X. Shizhong, Gigabit/s photonic generation, modulation, and transmission for a reconfigurable impulse radio UWB over fiber system, *IEEE photonics journa*l, 4: 805-816, 2012.

[19] . T. Abraha, C. Okonkwo, H. Yang, D. Visani, Y. Shi, H. D. Jung, E.Tangdiongga, T. Koonen, Routing of

power efficient IR-UWB wireless and wired services for in-building network applications, *Journal of Lightwave Technology*,30(11): 1651-1663, 2012.
[20] M. B. Menon, A. Gopakumar, N.V. Iqbal, A hybrid approach for UWB pulse shaping, *Proc. 2nd International Conference on Electronics and Communication Systems (ICECS),* pp. 373-377, 2015.
[21] S. T. Abraha, C. Okonkwo, H. Yang, D. Visani, Y. Shi, H. D. Jung, E.Tangdiongga, T. Koonen, Performance evaluation of IR-UWB in short range fiber communication using linear combination of monocycles, *J. Lightw. Technol.*,29(16):1143–1151, 2011.
[22] M.S. Munna, S. Tarannum, B. Barua, K. M. Rahman, IR-UWB transceiver for the detection of survivors buried in debris. *Proc. IEEE International Conference on Informatics, Electronics & Vision (ICIEV)*, pp. 1-7. 2015.
[23] R. A. Fayadh, F. Malek, A. H. Fadhil, N. Saudin , UWB selective rake receiver using multiple comparators. . *Proc. IEEE International Conference on Electronic Design (ICED)*, pp. 1-4, 2014.
[24] M. Mirshafiei, M. Abtahi, L. A. Rusch, Ultra-wideband pulse shaping: bypassing the inherent limitations of the Gaussian monocycle, *IET communications*, 6: 1068-1074, 2012.
[25] Z. Bai, J. Liu, Hsiao-Hwa Chen, Design of ultra-wideband pulses based on spectrum shifted Gaussian waveforms, *IET Communications*, 7: pp.512-520, 2013.
[26] S. K. Shaikhah, S. A. Mustafa, K. Al-sulaifanie Bayez, Performance Study of UWB System at Various Signal Parameters, *Indian Journal of Applied Research,* 5.9: 126-129, 2016.
[27] S. Mohammad, S. Sadough, A tutorial on ultra wideband modulation and detection schemes. *Shahid Beheshti University, Faculty of Electrical and Computer Eng,* Tehran, pp.1-22, 2009.
[28] S. Taran, D. Nitnaware, Performance Evaluation of 802.15.3a UWB Channel Model with Antipodal, Orthogonal and DPSK Modulation Scheme. *I.J. Wireless and Microwave Technologies*, 1: 34-42, 2016.
[29] K. R. Patel, R. Kulkarni, Ultra-Wideband (UWB) Wireless System. International *Journal of Application or Innovation in Engineering & Management*, pp. 1-15, 2014.
[30] K. Ayub, Z. Valerijs, Technology Implications of UWB on Wireless Sensor Network-A detailed Survey. *International Journal of Communication Networks and Information S*ecurity, 7: 147-161, 2015.